THE JOURNAL OF NAVIGATION (2005), **58**, 257–271.
doi:10.1017/S0373463305003231 Printed in the United Kingdom

Validation of Map Matching Algorithms using High Precision Positioning with GPS

Mohammed A. Quddus, Robert B. Noland, Washington Y. Ochieng

(*Imperial College London*)

(Email: w.ochieng@imperial.ac.uk)

Map Matching (MM) algorithms are usually employed for a range of transport telematics applications to correctly identify the physical location of a vehicle travelling on a road network. Two essential components for MM algorithms are (1) navigation sensors such as the Global Positioning System (GPS) and dead reckoning (DR), among others, to estimate the position of the vehicle, and (2) a digital base map for spatial referencing of the vehicle location. Previous research by the authors (Quddus et al., 2003; Ochieng et al., 2003) has developed improved MM algorithms that take account of the vehicle speed and the error sources associated with the navigation sensors and the digital map data previously ignored in conventional MM approaches. However, no validation study assessing the performance of MM algorithms has been presented in the literature. This paper describes a generic validation strategy and results for the MM algorithm previously developed in Ochieng et al. (2003). The validation technique is based on a higher accuracy reference (truth) of the vehicle trajectory as determined by high precision positioning achieved by the carrier-phase observable from GPS. The results show that the vehicle positions determined from the MM results are within 6 m of the true positions. The results also demonstrate the importance of the quality of the digital map data to the map matching process.

KEY WORDS

1. GPS. 2. Map matching. 3. High precision positioning. 4. Digital road network map.

1. INTRODUCTION. A range of transport telematics applications and services require continuous and accurate positioning information of vehicles travelling on a road network. Examples are in-car navigation systems, dynamic route guidance, fleet management, incident management, public transport management and on-board emissions monitoring systems. Many of these services also require the vehicle to be displayed on a map in real time without error. Two types of information are essential for such telematics applications and services. These are the determination of the vehicle position and the determination of the physical location of the vehicle on the mapped road network.

The vehicle positioning data is usually obtained from a range of navigation systems, such as Inertial Navigation Systems (INS), Dead Reckoning (DR) sensors,

ground-based (Terrestrial) radio frequency systems, Global Navigation Satellite Systems (GNSS) such as the Global Positioning System (GPS), and systems that employ more than one sensor such as GPS and DR (Quddus et al., 2003; Ochieng et al., 2003). GPS is widely used as a positioning sensor in land vehicle navigation. However, it is affected by both systematic errors or biases and noise (Ochieng et al., 2003). With the removal of the effects of selective availability (SA) in May 2000, GPS positioning accuracy has improved from 100 m (95%) to 15-20 m (95%). Despite this improvement, a real-world field test conducted in London showed that the GPS positioning errors sometimes could be offset from the true position by more than 50 m (Zhao et al., 2003). In a study in Hong Kong it was found to be off by more than 80 m (Chen et al., 2003). This is not surprising because positioning errors depend on the type of urban environment (which could result in poor quality measurements and weak satellite geometry) and the type of GPS receiver.

Another essential element for continuous and accurate positioning information of the vehicle is a digital map of the road network. Since the vehicle is essentially constrained to a finite network of roads, the road network map is used as a physical reference for the location of the vehicle. However, road network maps also have errors (Noronha and Goodchild, 2000). For example, roads are represented as a single ''centreline'' and curvatures are represented as piecewise linear lines (for gentle curves) or as a polyline (for sharp curves). This generalization alters the features on the ground and potentially introduces significant biases (NRC, 2002).

As a result of such inaccuracies in the positioning system and the digital base map, actual geometric vehicle positions do not always map onto the spatial road map, even when the vehicle is known to be on the road network. This phenomenon is known as spatial mismatch (NRC, 2002). Spatial mismatch is larger at junctions, roundabouts, complicated fly-overs and built-up urban areas with complex route structures. These environments also decrease the level of performance achievable with GPS.

Map matching (MM) algorithms are designed to place the vehicle on a link in a digital map. If both the vehicle location and the digital maps are perfectly accurate, the algorithm is simple and straightforward (Greenfeld, 2002). However, in most cases it is not possible to use simple algorithms due to the error sources identified above, thus requiring more sophisticated MM algorithms. The purpose of MM algorithms is twofold (a) the identification of a link among the possible links in the vicinity of the vehicle, and (b) the determination of the actual vehicle position on that link. Most studies (e.g., Bernstein and Kornhauser, 1996; Krakiwsky et al., 1988; White et al., 2000; Greendfeld, 2002; Taylor et al., 2001 etc) have not used error information associated with the positioning sensor and digital road network data in determining the vehicle location on a road segment.

Due to errors associated with the location data and the digital map data as described above, there is always a level of uncertainty associated with MM algorithms. No validation studies assessing the performance of MM algorithms have been reported in the literature. A MM algorithm can be validated using a higher accuracy reference (truth) of the vehicle trajectory. The objective of this paper is to develop a validation technique for MM algorithms using a reference trajectory determined from the high precision carrier-phase observable from GPS. The MM algorithm developed in Ochieng et al. (2003) and described briefly below, will be tested using the validation techniques developed here.

The paper is organized as follows. First we provide a brief description of the improved MM algorithms developed previously by the authors (Ochieng et al., 2003). The next section describes the basic principles of high precision positioning using the carrier-phase observable from GPS. This is followed by a description of the proposed generic validation methodology for MM algorithms. The next section describes the application of the validation technique to the new MM algorithms developed by the authors, followed by a presentation of the results. The paper ends with conclusions and recommendations for further avenues of study.

2. IMPROVED MM ALGORITHM.

A probabilistic approach was used to develop an improved MM algorithm by the authors in previous research fully described in Ochieng et al. (2003). This algorithm makes use of the positioning data from either stand-alone GPS or an integrated GPS/DR system. The integration of GPS and DR is performed using an Extended Kalman Filter (EKF) algorithm (described in Zhao et al., 2003). The key features of the MM algorithm are presented here.

Two distinct processes were developed for the identification of the correct link. These are (a) the *initial matching process* (IMP) and (b) the *subsequent matching process* (SMP). The function of the IMP is to identify a correct link for an initial position fix. Since the vehicle is expected to travel on this initial road segment for at least a few seconds, the subsequent position fixes are matched to this road segment. Therefore, after successfully identifying a correct link for an initial GPS or GPS/DR fix, the SMP starts matching the subsequent position fixes. In the SMP, the fixes are matched to the same road segment identified in the IMP if certain conditions exist, such as if the distance travelled is short, the difference in heading between fixes is low, and the vehicle does not cross any junctions (see Ochieng et al., 2003 for details). Otherwise, the algorithm goes back to the IMP and identifies a new road segment for the last non-matched position fix.

Assuming that the correct link has been identified as per the IMP and/or SMP, the physical location of the vehicle on the link can be determined in two ways with the available data. One method is to use map data (i.e., link heading) and vehicle speed from the positioning sensors. If an initial position for the vehicle is known then the vehicle position (easting, e_{map}, northing, n_{map}) can be derived epoch-by-epoch from the link heading and speed information. The other method is to adopt the perpendicular projection of the GPS or GPS/DR fix on to the link that results in the easting (e_{gps}) and northing (n_{gps}) coordinates. Since both methods are associated with errors, an optimal estimation procedure (combining the two methods) is used to determine the final location of the vehicle on the road segment.

The optimal easting ($\hat{e}$) and northing ($\hat{n}$) for a particular epoch are expressed as

$$\hat{e} = \left(\frac{\sigma^2_{gps,e}}{\sigma^2_{map} + \sigma^2_{gps,e}} \right) e_{map} + \left(\frac{\sigma^2_{map}}{\sigma^2_{map} + \sigma^2_{gps,e}} \right) e_{gps} \tag{1}$$

$$\hat{n} = \left(\frac{\sigma^2_{gps,n}}{\sigma^2_{map} + \sigma^2_{gps,n}} \right) n_{map} + \left(\frac{\sigma^2_{map}}{\sigma^2_{map} + \sigma^2_{gps,n}} \right) n_{gps} \tag{2}$$

where σ^2_{map} is the error covariance associated with map data, $\sigma^2_{gps,e}$ and $\sigma^2_{gps,n}$ are the easting and northing components of the error covariance associated with the navigation sensor. The error variance associated with $\hat{e}$ can now be expressed as

$$\frac{1}{\sigma^2_{mm,e}} = \frac{1}{\sigma^2_{map}} + \frac{1}{\sigma^2_{gps,e}} \tag{3}$$

where $\sigma^2_{mm,e}$ is the error variance associated with optimal estimation of $\hat{e}$. Note from equation (3) that $\sigma^2_{mm,e}$ is less than either σ^2_{map} or $\sigma^2_{gps,e}$. That is, the uncertainty in the estimation of the vehicle position using optimal estimation is decreased by combining two measurement methods. Similarly, the error variance associated with the optimal estimation of $\hat{n}$ can also be derived from equation (3). Ochieng et al. (2003) show examples of the superiority of this algorithm compared to previously developed algorithms in the literature.

3. HIGH PRECISION POSITIONING.

The two main GPS observations used for positioning are pseudo-ranges from code measurements (C/A code and P code) and carrier-phases (L1 and L2). The P-code is used to support the Precise Positioning Service (PPS) (10-20 m) and the C/A code the Standard Positioning Service (SPS) (20-30 m). For security concerns the P-code is encrypted (downgraded) to the Y-code so that only authorised users can access the code. This is known as Anti-spoofing (A-S). On the other hand, positioning solutions using carrier-phase measurements give a positioning accuracy at the centimetre level (Leick, 2004).

3.1. *The Carrier-phase Observable*.

The signals transmitted by GPS satellites consist of two carrier waves (L1 and L2). The L1 carrier has a frequency of 1575.42 MHz and a wavelength of 19 cm. The L2 carrier has a frequency of 1227.60 MHz and a wavelength of 24 cm. The carrier-phase observable is derived from the measurement of the difference between the phase of the signal arriving from the satellite, and the phase of the signal generated locally at the receiver. The direct measurement consists of a phase reading of the fractional part of the whole (*integer*) number of cycles in the range between the satellite and the receiver (Figure 1). Unfortunately, the receiver has no knowledge of the number of whole wavelengths at lock-on (either at the start or after loss of lock) but keeps count of the integer number of wavelengths to be added or subtracted as the receiver to satellite range changes. The whole number of cycles referred to as *integer ambiguity* must be resolved in order to determine the range between the receiver and the satellite.

The need to determine the resolution of the integer ambiguity arises from the desire to use carrier-phase ranges in the user position solution instead of pseudo-ranges. The use of carrier-phase ranges results both in improved *accuracy* and *precision*. This improvement is largely due to the different effects of some of the errors that affect the observables. The improvement in precision is mainly due to the difference in the effect of receiver thermal noise on carrier-phase and code-phase measurement errors. Improvement in accuracy is the direct result of the effect of multipath errors which are proportional to the wavelength of the signal. With the exception of the multipath bias and ionospheric delay bias which affects *code (pseudo-range)* and *carrier-phase* measurements in an equal but opposite sense, all other measurement biases associated with pseudo-ranges have an identical effect on the carrier-phase range. Hence

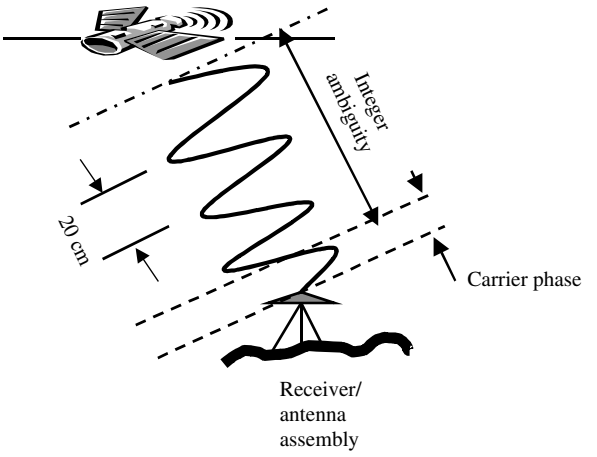

Figure 1. Carrier-phase and integer ambiguity.

well established principles and techniques used to reduce these biases in pseudo-range measurements can be applied to carrier-phase measurements to allow an accurate resolution of the integer ambiguities. After the treatment of the biases arising from satellite navigation errors, the only thing that remains in the derivation of the range between the satellite and receiver from carrier-phase measurements is the determination of the integer ambiguity.

Carrier-phase data processing is usually carried out in relative mode, between a static receiver at a known location and another receiver that is either static or moving. The effect of relative positioning (for limited baseline lengths) is to eliminate common errors and to reduce others significantly. The most commonly used observable in the relative mode is the double differenced (DD) observable where the satellite clock and receiver clock errors are eliminated and satellite orbit and atmospheric errors are largely reduced.

3.2. *Ambiguity Resolution.* The key to carrier-phase observables is the correct determination of integer ambiguity. As long as the connection between the receiver and the satellite is not broken, integer ambiguity remains constant while the fractional phase changes over time can be measured by the receiver. The loss of signal lock between a GPS satellite and a receiver is referred to as 'cycle slip'. If the signal lock is re-established, a new ambiguity exists and must be solved for separately from the original ambiguity. The complexity of ambiguity determination depends on the type of applications e.g., whether the survey mode is static or kinematic. A fuller description of ambiguity determination can be found in Sauer (2004). Kinematic positioning with carrier-phase data has been used to determine the vehicle trajectory as computed by the *SkiPro GPS post-processing software*™ by Leica Geosystems AG (2001).

Unsuccessful ambiguity resolution, when passed unnoticed, may lead to unacceptable errors in the positioning results. Normally when processing an individual baseline, two types of double difference solutions result. One is a float solution in which the ambiguities are solved as real numbers, instead of integers, and the other is a fixed solution in which the ambiguities are fixed by basically exploring those integers close to the float solution of the ambiguities. Under normal circumstances, the fixed solution is better than a float solution. In open spaces and in static surveys, a

fixed solution should be routine. However, float solutions cannot be avoided in kinematic surveys especially in built-up urban areas. The variance-covariance matrix of the least squares estimation of the ambiguities contains the information necessary to infer the quality and reliability of ambiguity estimation. The *SkiPro GPS post-processing package* gives a number of quality indicators for each position estimate, including the variance from the variance-covariance matrix. A threshold value for the standard deviation of the horizontal positioning can be used to select the float solution position estimates to use as reference or truth alongside ambiguity fixed position estimates.

4. VALIDATION STRATEGY FOR MM ALGORITHMS.

The input to MM algorithms is usually obtained from GPS SPS based on single frequency (L1) C/A code-ranging. The main reason is that the SPS is designed for civilian use. Furthermore, the receivers that support SPS are also relatively cheap. However, the positioning data from GPS C/A code measurements need to be augmented with a Dead Reckoning (DR) sensor in order to achieve continuous vehicle location data in some areas, especially urban areas with urban canyons, streets with dense tree cover, and tunnels (Ochieng et al., 2003). Although the integration of GPS and DR improves the level of coverage (ability to obtain a position fix), it does not improve accuracy (position fixing with a desired level of accuracy) when tracking vehicles (Zhao et al., 2003).

The output of a MM algorithm is the link on which the vehicle is travelling and the physical location of the vehicle on that link. In order to validate the results of a MM algorithm, a higher accuracy reference (truth) of the vehicle trajectory is essential. The reference of the vehicle trajectory is determined by the carrier-phase observables from GPS as explained in the previous section with a high degree of precision. From this reference trajectory, the actual (truth) link on which the vehicle is travelling and the correct physical location (at the centimetre level) of the vehicle on that link are then determined.

The next step is to compare the results (both the identification of the link and the physical location of the vehicle) obtained from the MM algorithm and the reference trajectory. Since the location data used in the MM algorithms and the reference trajectory is obtained from two different receivers, time synchronization is a crucial issue. This can be resolved if both sensors are based on the same time reference, such as GPS time or Coordinated Universal Time (UTC). It should be noted that GPS time was 13 seconds ahead of UTC time in 2004. Once time synchronization is achieved between the receivers, the comparison can be performed.

Figure 2 shows a road segment in which the vehicle position from GPS (C/A code-ranging) is denoted by the point D, the corresponding position estimated from the MM results (on the road centreline) is represented by the point A (x2, y2) and the true position of the vehicle from GPS (carrier-phase observable) is indicated by the point B(x1, y1) for a particular epoch t. Since the actual position of the vehicle at epoch t is at the point B, the error in the easting coordinate is AC and the error in the northing component is BC. The horizontal error at epoch t (HE_t), therefore, is given by,

$$HE_t = \sqrt{(x1 - x2)^2 + (y1 - y2)^2} \tag{4}$$

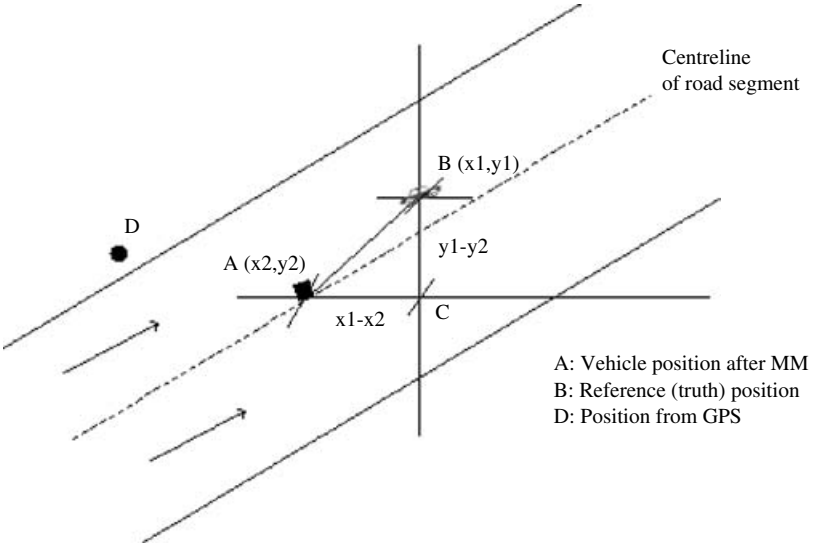

Figure 2. Determination of Error in MM.

A series of such horizontal errors can be derived using equation (4) for all epochs. The associated statistics derived from these errors (e.g., mean, standard deviation and RMS of the easting and northing component of the error) can be used to determine the relative performance of the MM algorithm.

Most of the road network map data contains only road centreline information. In this case MM algorithms use the centreline of the road segment as a reference and subsequently match the vehicle location data to it. Since the vehicle's actual position is not always constrained to be on the road centreline, a correction is required to the position of the vehicle matched onto the centreline.

In Figure 3, the line MN represents a road centreline on which the MM process matches a vehicle position at point A(x2, y2) at a particular epoch t. The corresponding true position of the vehicle at the same epoch is at point B(x1, y1). Line PQ (parallel to line MN) is drawn through point B. Point A is then orthogonally projected onto line PQ. Therefore, the final location of the vehicle position is at D (x, y) on the line PQ. Now the task is to determine the new easting, x, and northing, y, coordinate of the point D. The new easting coordinate is given by

$$x = x2 - CD = x2 - AB\cos(\theta + \alpha)\sin\theta \tag{5}$$

and the new northing coordinate is given by

$$y = y2 + AC = y2 + AB\cos(\theta + \alpha)\cos\theta \tag{6}$$

where θ can be derived from the heading of the road segment MN and can be obtained from the map data. The line AB is the known distance between A and B, and α can be derived from ΔAEB. The equations (5) and (6) are derived for a particular orientation of A and B (i.e., the true position and the position estimated from the MM results). For other orientations of A and B, these equations can be derived easily. The horizontal error after adjusting for the road centreline at epoch t (HE_{at}) is

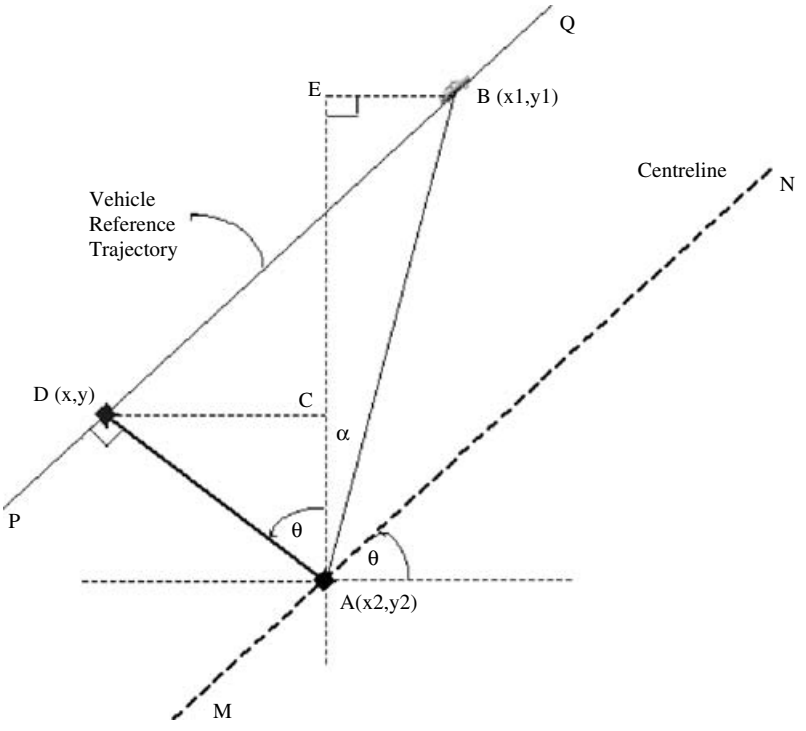

Figure 3. Corrections for Road Centreline.

therefore given by

$$HE_{at} = \sqrt{(x - x1)^2 + (y - y1)^2} \tag{7}$$

The difference between equations (4) and (7) can be viewed as the bias introduced by the MM algorithms for matching the location data on the road centreline.

5. APPLICATIONS AND RESULTS. The validation technique explained in the previous section was tested using the MM algorithm described above. The positioning data to assess the performance of the MM algorithm was obtained from a comprehensive field test in London on 5 July 2004. A vehicle was equipped with a navigation platform consisting of a 12-channel single frequency (L1) high sensitivity GPS receiver (for C/A code-ranging), a low-cost rate gyroscope and the interfaces required to connect to the vehicle speed sensor (odometer) and back-up indicator. In order to obtain the reference (truth) trajectory, the vehicle was also equipped with a 24-channel dual-frequency geodetic receiver with C/A code and P code-ranging. High accuracy local measurement of 3-D offsets between the two antennae was undertaken in order that the position information was referenced to a single point. The route was chosen carefully to have good satellite visibility as GPS carrier-phase observables require observations from a large number of GPS satellites for reliable and correct ambiguity resolution. The positioning data (easting and northing), speed, and heading were collected at a one second interval directly

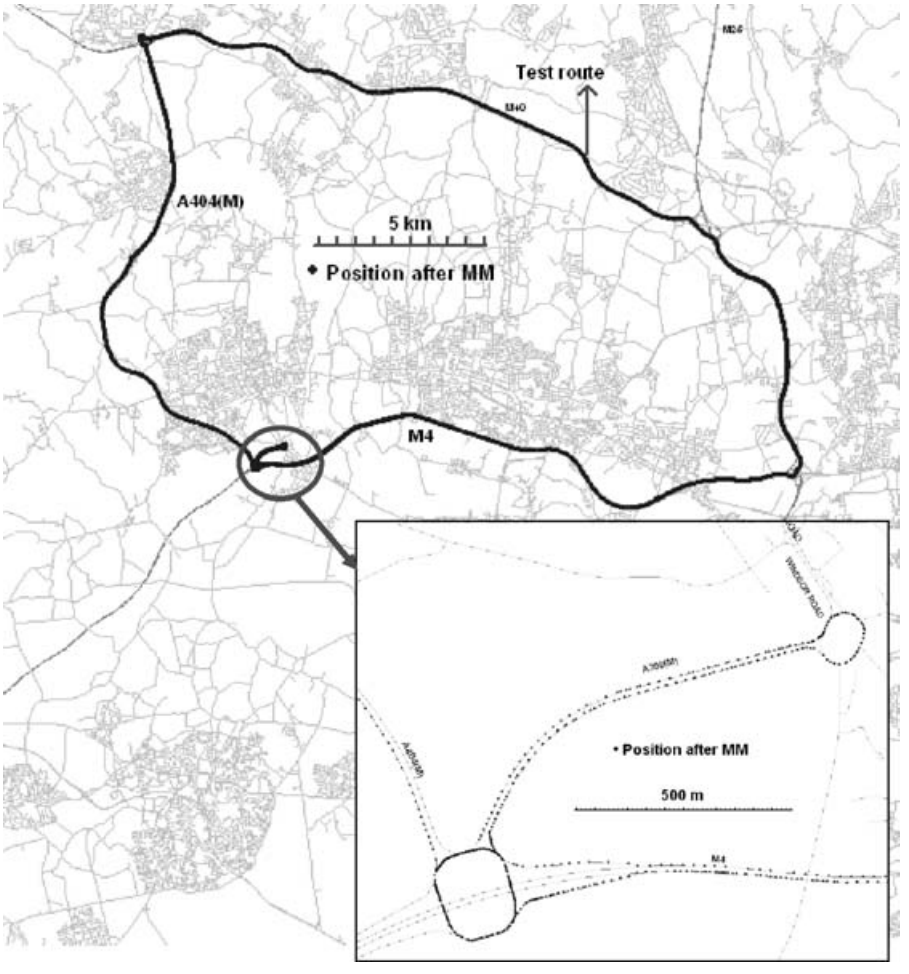

Figure 4. Test Route with Positions after MM.

from both GPS receivers. The duration of data collection was about 2 hrs. In order to implement the MM algorithm, the positioning data from GPS was augmented with DR. A high-resolution (1:2500) digital road network base map was used in the MM algorithm. The test route and the results after applying the MM algorithm are shown in Figure 4.

The GPS carrier-phase observables were processed in relative mode to reduce errors. Therefore, the raw data was needed from both a reference (static) station and also from the geodetic receiver (roving). The applicable static station for this study was 'LOND' (located in London) which is an Ordnance Survey (OS) active station operating within the *UK National GPS Network* (http://www.gps.gov.uk). The raw data from this station for 5 July 2004 (at a 5 second sampling interval) was extracted from the OS internet enabled data archives. All available data sets from the geodetic receiver and the reference station were processed in a *kinematic on-the fly* (KOF) post-processing mode using the *SkiPro GPS post-processing package*. The satellite

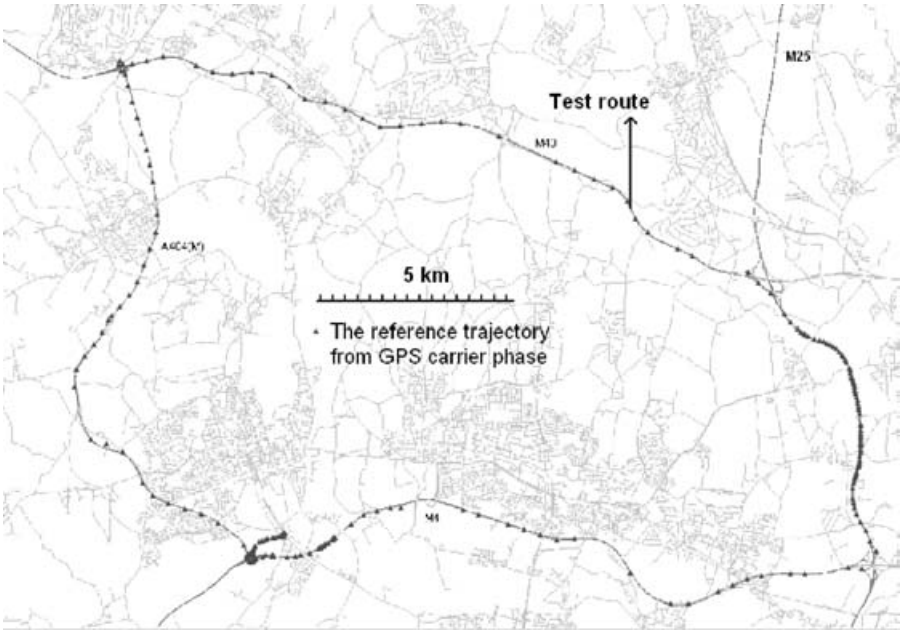

Figure 5. The Reference Trajectory of the Vehicle from the GPS Carrier-phase Observable.

positions were computed using broadcast ephemeredes[1]. The integer ambiguity (for GPS kinematic positioning) was resolved for all baselines involving all satellites in view (elevation angle cut-off 10^0), having detected and resolved all cycle slips at every 15 s intervals.

In our test route, both fixed and float solutions were obtained corresponding largely to open and built-up areas respectively. However, the positioning quality indicator in the form of the standard deviation of the horizontal position given by the *SkiPro GPS post-processing package* was used to select good float solutions used with the fixed solutions to provide the reference (truth) of the vehicle trajectory. It was found that the values of the standard deviation of the horizontal position were always less than 0.03 m if the positioning fixes were from the fixed solutions. In the case of the float solutions, this value varied from 0.4 m to 26.0 m. To select a threshold value for the standard deviation, which could identify good carrier-phase observations from the float solutions of the ambiguities, the position fixing data from both solutions was overlaid onto a high resolution digital base map (Figure 5). The positioning fixes from the float solutions were sometimes offset by more than 20 m from the road centreline when the standard deviation was large. It was found that the postioning fixes identified by a threshold value of 2.0 m agreed reasonably with the positioning fixes from the fixed solutions relative to the road centreline. Therefore, this threshold value of the standard deviation was employed to select all good carrier-phase observations from GPS.

[1] Ephemeredes are a set of parameters acquired by the receiver from the GPS signals to calculate the satellite position and clock offset.

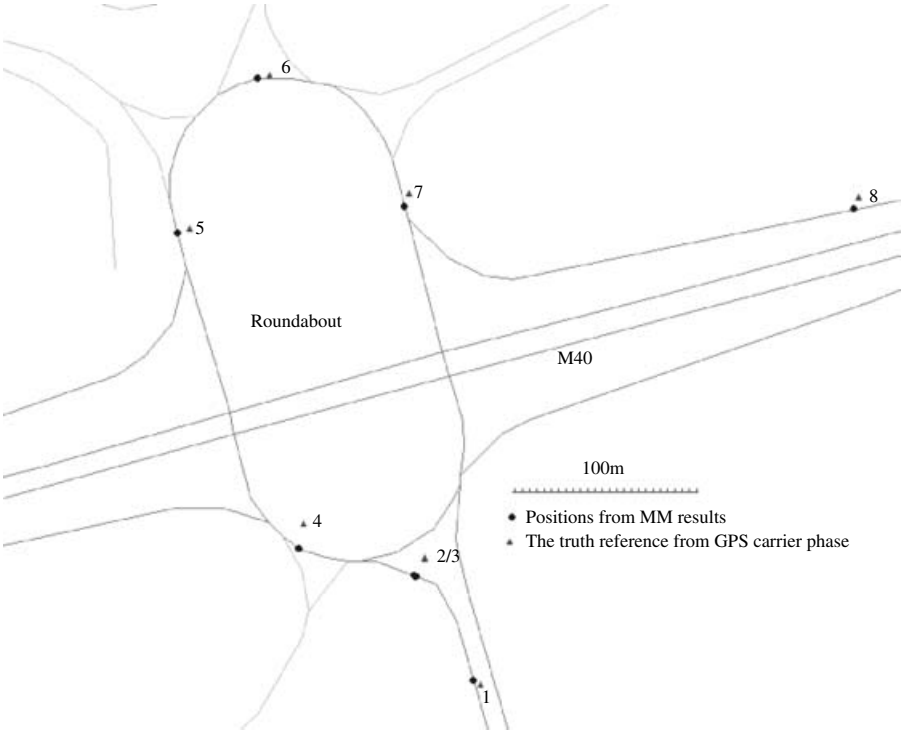

Figure 6. MM Results and the Truth Reference for a Particular Section of Test Route.

One section of the test route (on a roundabout) is shown in Figure 6. This includes the reference positions from the GPS carrier-phase observables (triangular symbols) and the corresponding positions estimated from the MM results (round dots). In this section of the route, the vehicle was travelling from points 1 to 8. In the real-world and for right-hand driving, the true positions of the vehicle should lie on the right side of the road centreline within points 1 to 5 and on the left side of the centreline within points 6 to 8. The reference positions (truth) from the GPS carrier-phase observations (triangular symbols) clearly agreed, confirming the quality of carrier-phase data. The discrepancies between the actual vehicle positions and the map are clearly apparent in Figure 6. None of the carrier-phase positions correspond exactly to the road network as drawn from the map database.

Based on the reference of the vehicle trajectory obtained from the GPS carrier-phase measurements, a set of correct links on which the vehicle was travelling was identified. Another set of links was identified for the corresponding epochs from the MM results. From this a 99.3% correct link identification was achieved by the new MM algorithm. In terms of physical location of the vehicle, different categories of horizontal positioning errors could be derived. The errors associated with the positions from the stand-alone GPS C/A code-ranging or the GPS C/A code-ranging augmented with DR are shown in Figure 7. The maximum horizontal error of this category was 34 m, i.e., all GPS positions were within 34 m relative to the true positions. The average error was 7.01 m and the standard deviation was 6.23 m. The

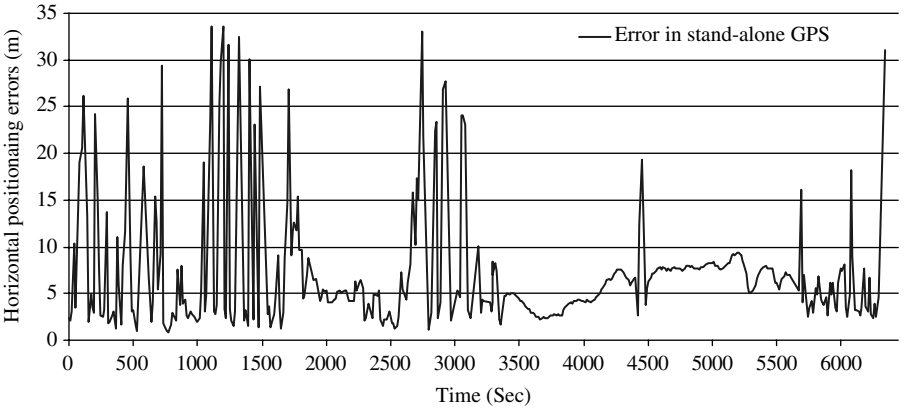

Figure 7. Horizontal Errors of Stand-alone GPS Positions Relative to the Reference (truth) of the Vehicle Trajectory.

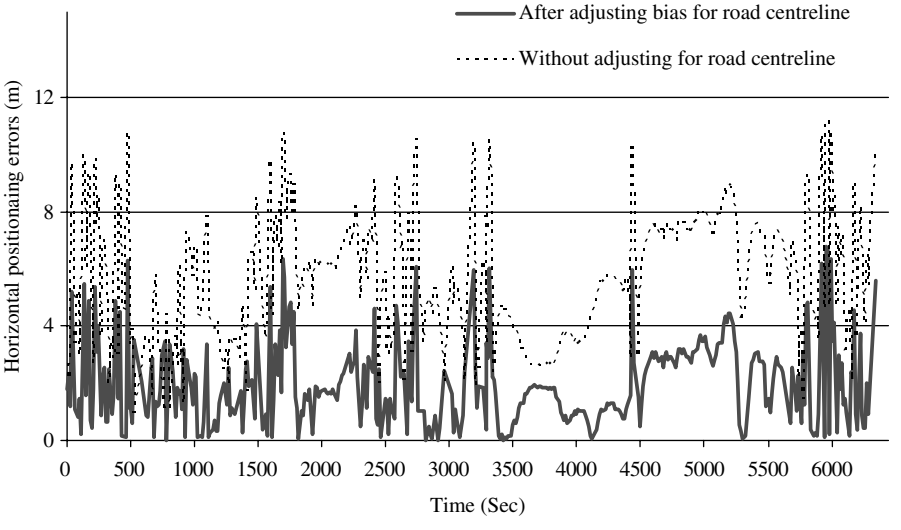

Figure 8. Horizontal Errors of Positions from the MM results Relative to the Reference (truth) of the Vehicle Trajectory.

root mean square (RMS) of the easting component of this error was 8.84 m and the northing component was 7.79 m.

The next step was to compute the horizontal errors associated with the positions estimated from the MM results. This is shown in Figure 8. The errors were calculated by equation (4). It was found that all MM positions on the road centreline were within 11 m (maximum error) of the true positions of the vehicle. The average of the errors was 5.6 m and the standard deviation was 2.26 m whereas the RMS of the easting component of the error was 5.12 m and the northing component of the error was 6.37 m. Therefore, a significant improvement in the estimation of the vehicle positions on the map was achieved by the MM algorithm. The horizontal errors were

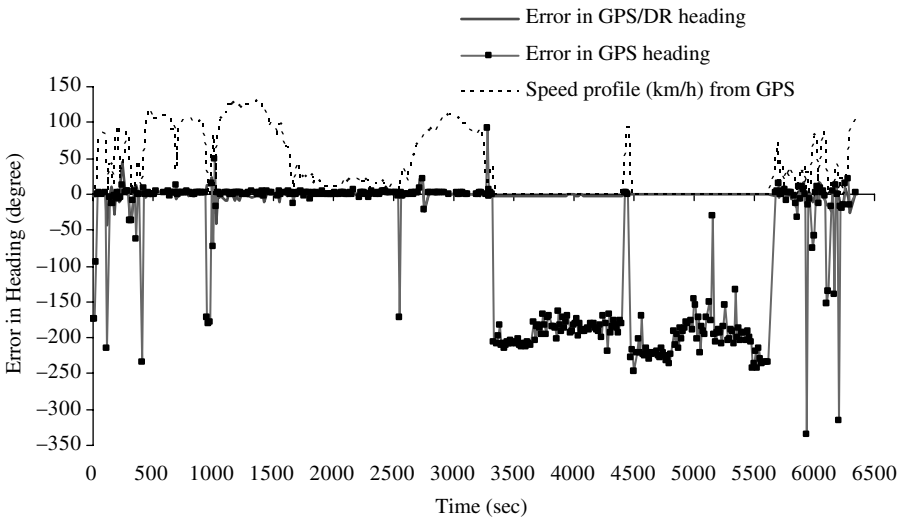

Figure 9. Errors in GPS and GPS/DR Heading Relative to the Truth Link Heading.

also calculated after correction for the road centreline using equation (7). This is also shown in Figure 8. The maximum horizontal error was only 6 m implying that the final positions of the vehicle were within 6 m of its true positions. The average of these horizontal positioning errors was 2.03 m and the standard deviation was 1.48 m. The RMS of the easting component of this error was only 3.03 m and the northing component was 4.03 m. Therefore, a further improvement in the estimation of the vehicle position could be achieved after adjusting for the road centreline. Clearly the quality of the vehicle positions estimated from the MM algorithm largely depends on the quality of the digital base map. If a good digital network map is not used in the MM process, the positions estimated from the MM process may be worse than the positions from stand-alone GPS.

Most of the MM algorithms in the literature (e.g., Greenfeld, 2002, White et al., 2000, Quddus et al., 2003) use epoch-by-epoch heading information from GPS in order to identify the correct link among the candidate links. Therefore, one can compare the GPS/DR heading with the actual link heading which is calculated from the map data whereas the actual link is identified by the GPS carrier phase observations. The results are shown in Figure 9. It was found that the heading from the stand-alone GPS was significantly different from the true heading. The difference was higher when the speed of the vehicle was very low. On the other hand, the vehicle heading from the integration of GPS/DR was very close to the true heading. Therefore, the heading derived from the stand-alone GPS SPS should be used with caution within MM algorithms.

6. CONCLUSIONS. A validation strategy to assess the performance of MM algorithms has been developed in this study. High precision positioning using GPS carrier-phase observables was employed in the validation methodology. Although the proposed validation technique is generic, it has been applied to an improved probabilistic MM algorithm, which was briefly described. The validation results revealed

that about a 99.3% correct link identification was achieved by the MM algorithm. It was found that the horizontal position of the vehicle estimated from GPS C/A code-ranging deviated at most by 34 m from its true positions, with an average error of about 7 m. The horizontal position of the vehicle was 11 m from its true position after the application of the MM algorithm indicating that MM improved the mapping of vehicle positions on a link. The average horizontal error was 5.6 m. The estimate was further improved to within 6 m in the estimation of the vehicle positions after adjusting MM results for the road centreline, with an average error of 2 m. One of the interesting findings was that the matching of the vehicle positions on the road centreline introduced additional error. If a good digital map is not used in MM algorithms, the estimation of the vehicle positions may become worse than the positions from GPS C/A code-ranging. Another finding was that the vehicle heading derived from the stand-alone GPS was significantly different from the true heading of the link especially at very low speed. Therefore, headings derived from GPS/DR must be used carefully in MM algorithms.

Future research will consider the integrity of map matching. This will include the specification of a metric for measuring the quality (and level of confidence of map matching) and the detection of anomalies (in raw and positional data).

ACKNOWLEDGEMENTS

The authors would like to thank Robin North and Shaojun Feng (both of the Centre for Transport Studies at Imperial College London) for their contribution to this study.

REFERENCES

Bernstein D., Kornhauser A. (1996). *An introduction to map matching for personal navigation assistants*. New Jersey TIDE Center. http://www.njtude.org/reports/mapmatchintro.pdf. Accessed June 19, 2002.

Chen, W, YU, M., LI, Zhi-lin, CHEN, Yong-qi (2003) Integrated Vehicle Navigation System for Urban Applications. *GNSS 2003*, Graz, April 2003, CD-ROM, 15 pp.

Greenfeld, J. S. (2002) Matching GPS observations to locations on a digital map. In proceedings of the 81st *Annual Meeting of the Transportation Research Board*, *National Research Council*, Washington D.C., 2002.

Hoffmann-Wellenhof, B., Collins, J., and Lichtenegger, H. (1997) *GPS theory and practice*, Springer-Verlag, New York, 1997.

Kaplan E. D. (1996) *Understanding GPS: Principles and Applications*, Artech House, London.

Krakiwsky, E. J., Harris, C. B., Wong, R. V. C. A (1988) Kalman filter for integrating dead reckoning, map matching and GPS positioning. In: *Proceedings of IEEE Position Location and Navigation Symposium*, 39–46.

Leica Geosystems AG (2001) *User guide v 2.1: SkiPro GPS post-processing software*, Roosendaal, The Netherlands.

Leick, A. (2004) *GPS Satellite Surveying*, Third Edition, John Wiley & Sons.

National Research Council (2002) *Collecting, processing and integrating GPS data into GIS*. NCHRP Synthesis 301. National Academy Press; Washington D.C.

Noronha, V. and Goodchild, M. F. (2000) Map accuracy and location expression in transportation-reality and prospects. *Transportation Research C*, **8**, 53–69.

Ochieng, W. Y., Quddus, M. A. and Noland, R. B. (2003) Map-Matching in Complex Urban Road Networks, *Brazilian Journal of Cartography* (*Revista Brasileira de Cartografia*), **55** (2), 1–18.

Ochieng, W. Y., Sauer, K. (2001) Urban road transport navigation requirements: performance of the global positioning system after selective availability. *Transportation Research Part C*, **10**, 171–187.

Quddus, M. A., Ochieng, W. Y., Zhao, L., Noland R. B. (2003). A general map matching algorithm for transport telematics applications. *GPS solutions*, **7(3)**, 157–167.

Sauer, K. (2004) *Integrated high precision kinematic positioning using GPS and EGNOS observations*, PhD dissertation, Imperial College London, UK., 2004.

Taylor, G., Blewitt, G., Steup, D., Corbett, S., Car, A. (2001) Road reduction filtering for GPS-GIS navigation. *Proceedings of 3rd AGILE Conference on Geographic Information Science*, Helsinki, Finland, 114–120, 2001.

Townsend, B. R., Nee, D. J. R. V., Fenton, P. C., and Dierendonck, K. J. V. (1995) Performance evaluation of the multipath estimating delay lock loop, in ION Navigational Technical Meeting, Anaheim, California.

White, C. E., Bernstein, D., Kornhauser, A. L. (2000) Some map matching algorithms for personal navigation assistants. *Transportation Research Part C*, **8**, pp. 91–108.

Zhao, L., Ochieng, W. Y., Quddus, M.A and Noland, R. B. (2003) An Extended Kalman Filter algorithm for Integrating GPS and low-cost Dead reckoning system data for vehicle performance and emissions monitoring. *The Journal of Navigation*, **56**, 257–275.